Journal of Luminescence 272 (2024) 120655

Contents lists available at ScienceDirect

Journal of Luminescence

journal homepage: www.elsevier.com/locate/jlumin

Full Length Article

Improved relative gain in Nd^{3+}doped GeO_2-PbO glass with double waveguides irradiated by femtosecond laser micromachining and decorated with Au nanoparticles

Camila D.S. Bordon [a,*], Jessica Dipold [b], Thiago F. Vecchi [a], Niklaus U. Wetter [b], Wagner de Rossi [b], Anderson Z. Freitas [b], Luciana R.P. Kassab [c]

[a] Departamento de Engenharia de Sistemas Eletrônicos, Escola Politécnica da Universidade de São Paulo, Av. Prof. Luciano Gualberto, 158, Travessa 3, São Paulo, SP, Brazil
[b] Instituto de Pesquisas Energéticas e Nucleares, IPEN-CNEN, 2242, Av. Prof. Lineu Prestes, São Paulo, SP, Brazil
[c] Faculdade de Tecnologia de São Paulo, CEETEPS, Praça Cel. Fernando Prestes, 30, São Paulo, SP, Brazil

A B S T R A C T

The paper explores the effects of Au nanoparticle (NP) islands deposited by sputtering technique on the surface of Nd^{3+}-doped GeO_2-PbO glasses, with double-line waveguides, produced via femtosecond laser processing for photonics. A Ti:sapphire femtosecond laser operating at 800 nm was employed to inscribe the waveguides directly into the glass, 0.7 mm beneath the surface. These waveguides were structured as pairs of parallel lines separated 10 μm. Additional procedures were undertaken to position the waveguides on the glass surface where Au NPs were deposited. Refractive index change of 10^{-3} at 632 nm was observed in both horizontal and vertical directions. Similar results for the beam quality factors (M_x^2 and M_y^2) at 632 nm and 1064 nm indicated x, y-symmetrical guiding. Photoluminescence and relative gain growth were observed due to Au NP islands. The relative gain reached 3.0 dB/cm representing an increase of approximately 450 % when compared to samples without the Au NP islands, and was attributed to the local field growth in their vicinities. This study highlights the potential to change Nd^{3+}-doped GeO_2-PbO glasses optical properties with Au nanoparticle islands, opening up new and promising prospects for photonics and 1064 nm optical amplifiers.

1. Introduction

Waveguides fabricated with femtosecond (fs) lasers have emerged as an innovative technology in modern photonics and optical communication systems. Femtosecond lasers have opened up remarkable opportunities in the design and fabrication of waveguides with high precision and control.

Glasses, as amplifying media, represent a significant category of host materials for rare-earth elements, with Nd^{3+} being a prominent example. Moreover, glasses are known for their ease of manufacturing and excellent optical finishing [1].

In the last two decades, bulk waveguide structures have emerged as a complementary combination of solid-state bulk lasers and fiber lasers, with compact geometries [2]. Direct femtosecond (fs) laser writing has gradually become one of the most popular methods in recent years. The fabrication of three-dimensional waveguides in glasses through femtosecond laser writing was first demonstrated in 1996 [3]. Ultra-short laser pulses have been extensively researched for their effects on glasses, with the goal of developing various photonic applications. Effective femtosecond laser writing of waveguides, with pulse repetition rates ranging from 1 kHz to 1 MHz and pulse durations of 45–180 fs, has been reported in various glass matrices such as silicates [4,5]; borates [5,6]; fluorides; chalcogenides [5]; phosphates doped with Er^{3+}/Yb^{3+} [7]; heavy metal oxides like tellurites doped with Er^{3+} [8], Er^{3+}/Ce^{3+}/Yb^{3+} [9] and La^{3+} [10], and undoped [11] and Yb^{3+} [12], and Yb^{3+}/Er^{3+} [13] -doped germanates.

Among the heavy metal oxide glasses, glasses of the germanate family have been little explored and have an intriguing response to fs laser pulses. Due to the increased photosensitivity properties of germanium, GeO_2-based glasses allow the formation of waveguides with a high contrast index [14].

When combined with heavy metal oxides, such as lead, germanate glasses achieve high values in various properties. These include density, thermal expansion, corrosion resistance, wide transmission window (UV to IR - 400 to 5000 nm), ultra-fast response time, low phonon energy (~800 cm^{-1}), and high linear (~2.0) and non-linear refraction indices [15,16]. Lead germanate glasses can exhibit excellent thermal stability and show no devitrification phenomenon throughout the temperature range from the glass transition temperature to the melting temperature [17]. Unlike silica glass, these glasses are transparent beyond 2 μm,

* Corresponding author.
E-mail address: camiladsb@usp.br (C.D.S. Bordon).

https://doi.org/10.1016/j.jlumin.2024.120655
Received 11 January 2024; Received in revised form 22 April 2024; Accepted 29 April 2024
Available online 30 April 2024

while silica glass becomes opaque. Heavy metal oxide glasses based on GeO_2 are also good hosts for rare earth ions, as they can incorporate a large amount of rare earth ions without agglomeration [15]. All these particular properties make them suitable hosts for the manufacture of non-linear optical devices, laser amplifiers, among various components used in IR applications [16].

Waveguide devices doped with Nd^{3+} ions may be suitable for providing optical gain in integrated optical applications, for example, lossless data transmission in optical interconnections and telecommunications, signal enhancement in integrated Raman spectroscopy or integrated lasers in opto-fluidic chips [18]. The incorporation of neodymium ions into germanate glass matrices introduces unique optical properties, such as laser emission at specific wavelengths, which has significant implications in various fields like telecommunications, optical amplification systems, and solid-state laser technology. Femtosecond laser pulses have been used to perform laser writing in glasses doped with Nd^{3+} ions, including phosphate [19] and silicate [20] glasses. These materials have shown promise for optical device applications, despite being relatively unexplored thus far.

There are two types of permanent modifications in materials induced by femtosecond laser pulses: in one of them, usually used in the manufacture of single-track waveguides, a smooth positive change in refractive index takes place, forming optical waveguides using low-energy pulses. The other type creates a negative refractive index change in the laser-exposed region, while the surrounding glass remains unchanged, and has been reported in some germanate crystals [21], germanate glasses [13] and tellurites [22]. Single-line waveguides offer the advantage of simpler and faster processing and have been successfully demonstrated in various glasses [4–6]. However, for materials with properties that do not allow effective confinement and propagation of light through a single-track, double-line waveguides present an alternative technique. The focus of the present work is on the application of modification due to the results previously achieved with double-line waveguides [11,13,23,24]. This approach was chosen after evaluations of both types of waveguides in previous experiments [11]. Despite testing a wide range of laser parameters, no guidance was observed in GeO_2-PbO glasses with a single line [11].

In this study, a dual waveguide was created by overlaying eight coinciding lines to form each of the two parallel lines. This method was developed to address the issue of neodymium absorption at 800 nm, which resonates with the fs laser's emitting wavelength, causing localized heating in the medium due to its non-optical decay [23]. This innovative approach applied faster writing speeds of 0.5 mm/s compared to the previous method (Er^{3+}/Yb^{3+}-doped GeO_2-PbO), which inscribed a single double line at a slower speed of 0.06 mm/s [13]. Slower speeds can lead to heat accumulation and glass fracture due to the resonance of neodymium absorption with the fs laser's wavelength. To mitigate this, writing each line of the double guide was divided into eight steps. This meant that the same total number of pulses per unit length was deposited on the glass through eight overlaps, each of which had low pulse density, achieved by increasing the laser beam's scanning speed. A high total number of pulses overlapping is necessary for the intended refractive index change, therefore, several lines were superimposed with sufficient intervals between each line to allow for cooling [13]. An interval of 40 s was provided between writing each line to ensure adequate cooling of the processed region. For neodymium-doped glasses, the phonon decay time is mostly in the range of nanoseconds to microseconds whereas our interval time is 40 s. This much longer interval time allows for dispersion of the locally accumulated heat. This cooling time is crucial due to the strong absorption of the laser-writing wavelength and the nonlinear absorption process typical of fs laser processing. As a result, each line consisting of eight superimposed lines has a density of 1,152 pulses overlapping within the laser's calculated focal point diameter inside the glass of 7.2 μm (without considering possible nonlinear phenomena in the beam propagation within the glass). By employing this innovative technique, significant internal gains of 5.56 dB/cm [23] and 8.5 dB/cm [24] at 1064 nm were achieved for eight superimposed lines in Nd^{3+}-doped GeO_2-PbO glass without and with Ag NPs, respectively. These outcomes prompted ongoing exploration that adopts the dual-line methodology in Nd^{3+}-doped GeO_2-PbO glass with gold (Au) nanoparticles (NPs) deposited on the surface of the double waveguide by RF Magnetron Sputtering technique.

Metallic NPs can have a positive influence on the luminescence of rare-earth ions (REIs). In experiments conducted by Anger [25], an increase in luminescence was observed for distances ranging from 5 nm to 20 nm between NPs and REIs, due to the enhancement of the local field and energy transfer from NPs to rare-earth ions. For distances smaller than 5 nm, luminescence was reduced, likely due to energy transfer from REIs to NPs, making non-radiative relaxations dominant [25,26]. Doped glasses with neodymium and metallic NPs, such as Ag and Au, had their luminescence increased when excited at 808 nm due to the enhanced local field effect in the vicinity of the NPs, which increases the density of excited Nd^{3+} ions [27–29]. In pedestal waveguides fabricated from amorphous thin films co-doped with Tm^{3+}/Yb^{3+} [30] and Yb^{3+}/Er^{3+} [31] in PbO-GeO_2, the internal gain at 805 nm was significantly enhanced due to the incorporation of Au NPs obtained by RF Magnetron Sputtering deposition.

In this study, we present for the first time the influence of Au NPs islands on the optical properties of Nd^{3+}-doped GeO_2-PbO glasses, with waveguides produced by the aforementioned dual-line methodology processed by fs laser. The Au NPs were deposited on the surface of Nd^{3+}-doped GeO_2-PbO glass by RF Magnetron Sputtering technique and led to significative relative gain enhancement, at 1064 nm, attributed to the plasmonic effects of Au NPs islands. The results obtained are relevant for the development of new optical amplifiers.

2. Materials and methods

2.1. Glass preparation

To the glass composition containing 40 wt% GeO_2 and 60 wt% PbO, it was added 0.5 wt% of Nd_2O_3. To fabricate the glass, the melt-quenching technique was employed at a melting temperature of 1200 °C. Alumina crucible was used to melt the mixture, which was then poured into preheated brass molds. The glass was annealed at 420 °C for 1 h to minimize internal stress. After cooling within the furnace and final polishing, samples with a thickness of 2 mm and parallel faces were prepared for the experiments.

2.2. Waveguide production

In this study, a focused femtosecond (fs) Ti:sapphire laser was used to fabricate the waveguide. The laser had a pulse duration of 30 fs, a maximum energy per pulse of 200 μJ, and operated at a repetition rate of 10 kHz. To avoid damage to the sample surface, and at the same time obtain a guide with long walls, a lens with a low numerical aperture (NA ~ 0.23) was used and its focus was placed at a relatively high depth. Thus, the laser beam was focused 0.7 mm below the surface, using a lens of 20 mm focal length. During the inscription process, the laser beam, delivering 30 μJ of energy per pulse, was focused perpendicular to the polished surface of the sample. Its linear polarization was tilted at a 45° angle relative to the direction of movement. A pair of parallel lines with a 10 μm spacing between them were written, with each line consisting of 8 coincident lines as explained previously. Our previous works [23,24] used the same processing parameters.

After femtosecond laser writing, a thinning process was carried out using the ULTRAPOL Fiber Lensing Machine polisher, so that the waveguides could be positioned on the surface of the glass sample.

2.3. Gold deposition procedure

The Magnetron Sputtering technique was used to obtain Au NPs. To

achieve this, a commercial gold metal target was used to deposit gold onto the glass surface. The sputtering process lasted for 2.5 min, with 5 W applied to the target electrode. The low power and time requirements helped to incorporate small concentrations of gold onto the glass for nanoparticle formation, as high concentrations could compromise light guidance. Fig. 1 illustrates the final profile of the double waveguide with Au NPs on the surface and the configuration used for waveguide processing.

2.4. Characterization

Optical microscopy measurements were conducted in the waveguide region using a LabRam HR Evolution—HORIBA and a Leica DMLP polarizing light microscope equipped with a MC170 HD camera, and the near field beam profile (at a wavelength of 632 nm) was captured using a CCD camera.

The experimental setup for measuring the Numerical Aperture (NA) is presented in Fig. 2. The characterization of the numerical aperture (NA) measures the ability of the waveguide to collect light and transmit it efficiently; it is related to the difference in refractive index between the core of the waveguide and the medium that surrounds it. The approximation between numerical aperture and refractive index is appropriate for identifying the optical performance of the waveguide through its properties. The numerical aperture was determined as follows [32].

$$NA = \sqrt{n_1^2 - n_2^2} \approx \sqrt{\sim 2n_2\Delta n} \tag{1}$$

where n_1 and n_2 represent the refractive index of the core and the cladding, respectively, Δn represents the refractive index difference and NA is given by the following equation [32]:

$$NA = n.sen\theta \tag{2}$$

In the equation above, n represents the refractive index of the medium in which the wave propagates, and θ denotes the beam divergence angle in the far field which can be calculated using the following trigonometric relationship:

$$sen\theta = \frac{w(z)}{\sqrt{z^2 + w(z)^2}} \tag{3}$$

The numerical aperture of the waveguides was determined by measuring the divergence angle of the output beam in the far field at 632 nm (θ) (see Fig. 2). This was accomplished by measuring the output beam's diameter at various distances.

The M^2 factor is a parameter used to measure the quality of the output laser beam from a waveguide, as proposed by Anthony E. Siegman in the 1990s [33]. M^2 measurements were obtained at 632 nm by focusing the output signal from the waveguide with a plan-convex lens and measuring the beam diameter (2 w) at various positions from the near to the far field. The experimental data were adjusted by the equation below, and provided the values for M_x^2 and M_y^2:

$$d = d_0\sqrt{1 + \left(\frac{(M^2\lambda(Z - Z_0))}{(\mu\ {d_0}^2)}\right)^2} \tag{4}$$

In the equation above, $d = 2\ w$, and $d_0 = 2\ w_0$.

By applying the equation provided below [34], we determined the M^2 value at 1064 nm:

$$M^2 = \frac{\theta_{ideal}.w_{0ideal}.\pi}{\lambda} \tag{5}$$

The half-angle beam divergence (θ_{ideal}), obtained from M^2, and the Gaussian beam waist radius (w_{0ideal}) were both measured at 632 nm using the experimental setup of Fig. 2.

A propagation loss measurement was performed using the Cutback method [23,35] at a wavelength of 1064 nm, with the support of a power meter. The equation employed for the calculation is the following:

$$\alpha\left[\frac{dB}{cm}\right] = -10\frac{log\left(P_2/P_1\right)}{(d_2 - d_1)} \tag{6}$$

In the equation above P_2 and P_1 are the powers related to the different lengths of the samples, d_2 an d_1, respectively.

The photoluminescence (PL) measurements were made by exciting the sample with a continuous-wave laser operating at 808 nm, as shown in Fig. 3 (a). The PL signal was collected in the same direction of the incident beam and analyzed by a spectrophotometer. A vertical scan was carried out at two different distances. The first measurement was carried out at 0.8 mm distance from the Au NPs islands deposited on the surface (Fig. 3 (b)) whereas and the second one (Fig. 3 (c)) was performed very close to the Au NPs surface (thickness sample of 1.3 mm).

The relative gain (G) was calculated using Equation (7) [13,23,24,35]. In this equation, P_{signal} represents the signal measured at the sample output with the signal laser active (at 1064 nm) and the pump laser (at 808 nm) inactive, while P_{ASE} corresponds to the amplified spontaneous emission (ASE) when only the pump laser is active. When both the pump and probe lasers were active, the combined power, $P_{signal+ASE}$, was obtained. The signal of the stimulated emission (SE) at 1064 nm is represented by $P_{signal+ASE} - P_{ASE}$, and the sample length (0.8 cm) is denoted by d. Fig. 4 illustrates the configuration used for this characterization.

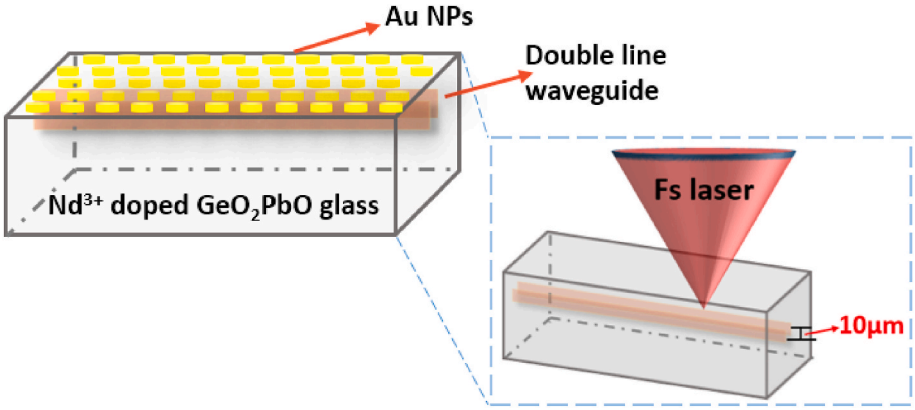

Fig. 1. Illustrations of Nd^{3+} doped GeO_2PbO double waveguides with Au NPs islands and the configuration employed for dual waveguide fabrication.

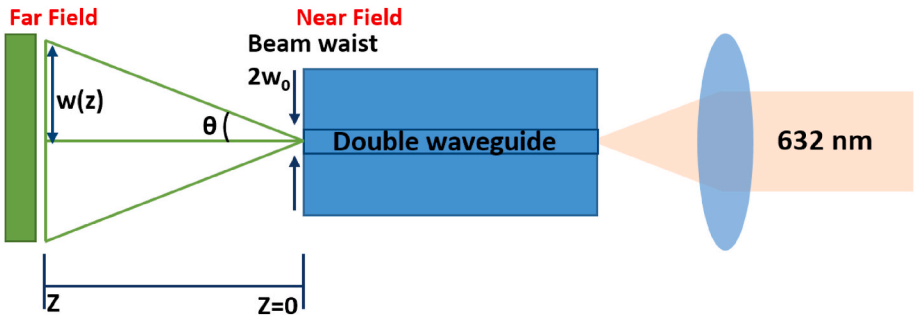

Fig. 2. Experimental setup for numerical aperture (NA) estimation based on the far-field beam divergence angle, θ.

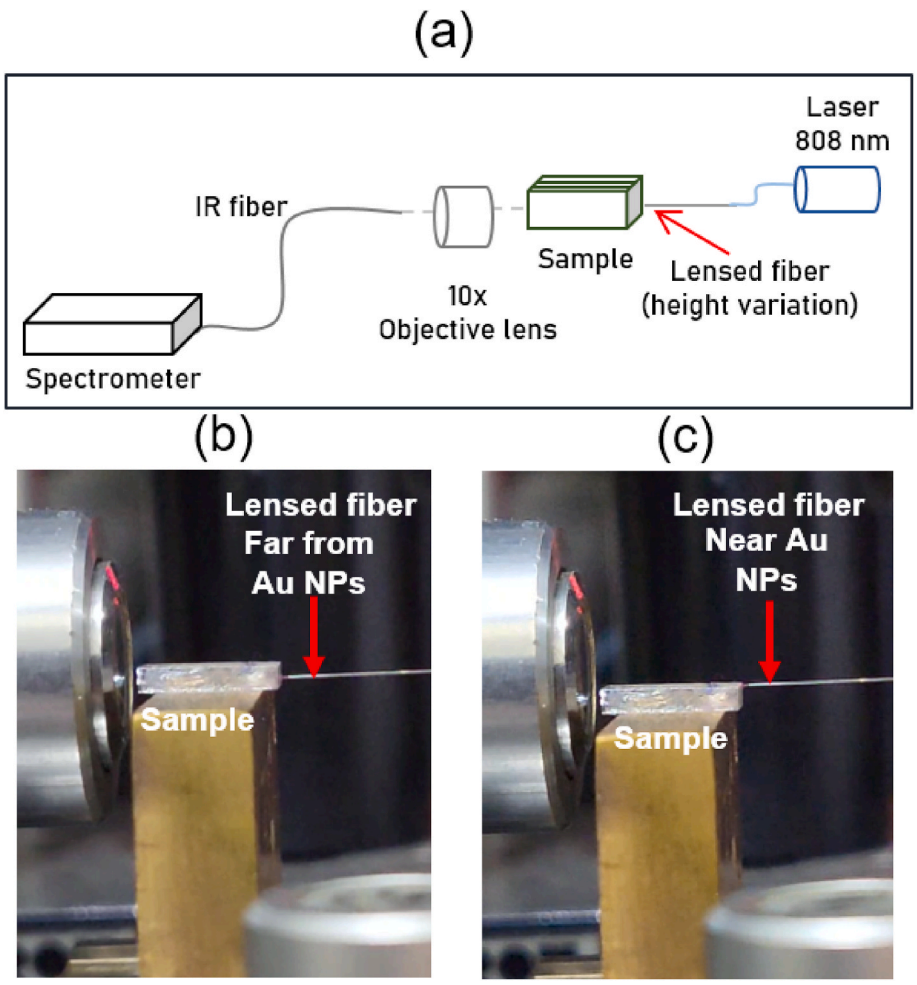

Fig. 3. (a) Experimental setup used for photoluminescence measurement; (b) and (c) Images illustrating measurements taken at two different heights of the sample (0.8 mm from Au NPs and close to Au NPs).

$$G\left[\frac{db}{cm}\right] = \frac{10 \times log\left(\left(P_{signal+ASE} - P_{ASE}\right) / P_{signal}\right)}{d} \quad (7)$$

The objective of the Atomic Force Microscopy (AFM) technique is to generate a topographic image of a material's surface and determine the distribution of Au NPs by scanning it with a probe. The AFM measurements were conducted using a HORIBA OmegaScope AFM operating in tapping mode using a Si tip.

3. Results

To investigate the spatial distribution of Au NPs within the core surface of the waveguides, AFM technique was performed. In Fig. 5, AFM images (Fig. 5 (a) and (b)) and the corresponding size distribution results (Fig. 5 (c)) of Au NPs on the surface of Nd^{3+} doped GeO_2-PbO glass are presented together with the schematic figure of the glass sample. From analysis performed on the image in Fig. 5 (a), Au NPs ranging in size from 5 to 45 nm were found as represented in the distribution graph (Fig. 5 (c)). Fig. 5 (b) shows a 3D image (a magnification from Fig. 5 (a)) where it becomes evident the surface roughness generated after the gold deposition.

Fig. 5 (d) presents the top image, captured using optical microscopy, which displays dual waveguides inscribed onto Nd^{3+}-doped GeO_2-PbO glass with the eight superimposed lines separated by a 10 μm distance.

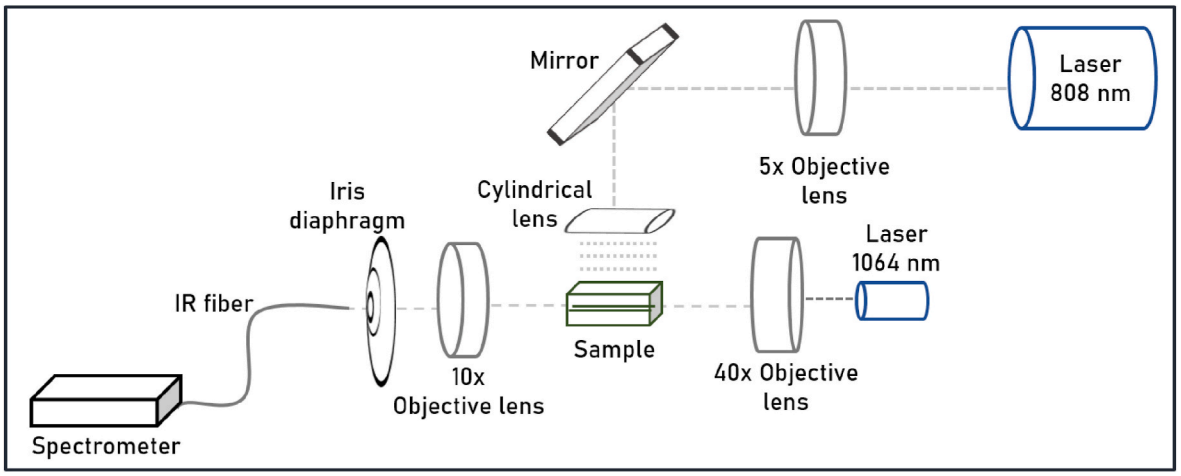

Fig. 4. Experimental setup used for relative gain measurements at 1064 nm and excitation at 808 nm.

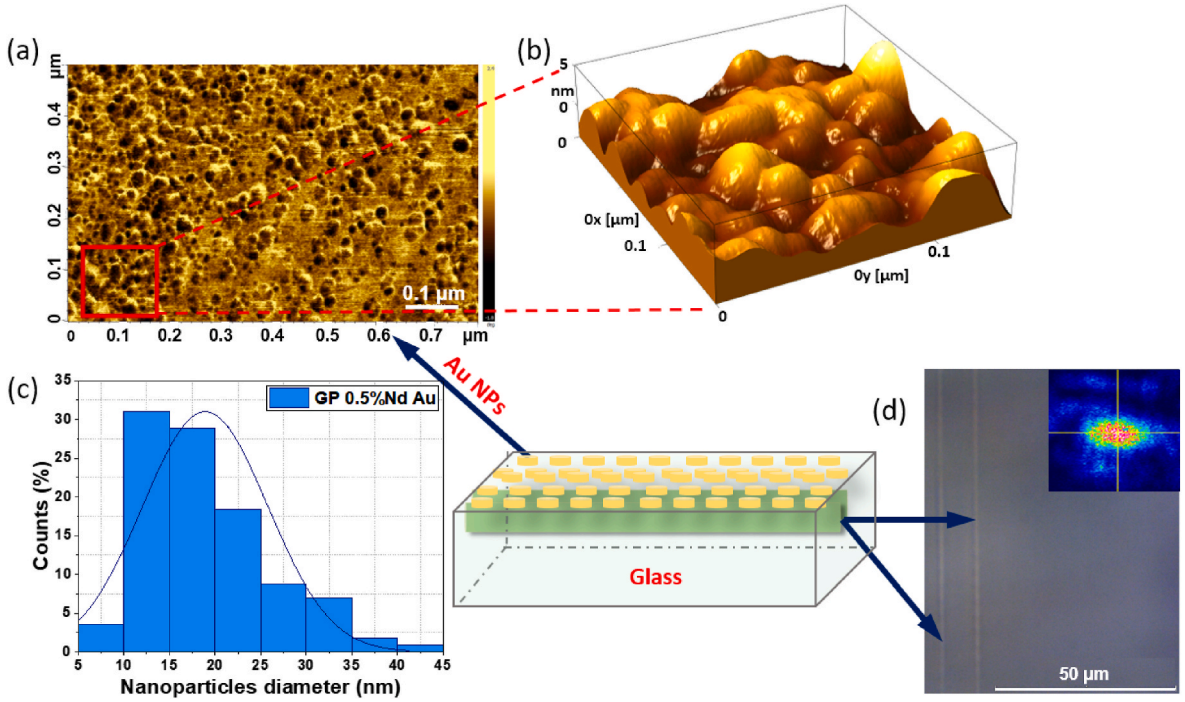

Fig. 5. a) 2D and b) 3D (magnification from 2D image) atomic force microscopy image of Au NPs deposited on the surface of Nd^{3+} doped GeO_2-PbO sample; c) distribution of Au NPs size on the glass surface; d) top view microscope image of the double line waveguide in Nd^{3+}-doped GeO_2-PbO glass; the near field beam profile (at 632 nm) is presented in the inset. The image in the center of the figure shows a schematic of the glass sample with waveguides written by fs laser and Au NPs islands on its surface.

Each written line appears to have a visual width of 2 µm. The inset in the figure reveals mode images at 632 nm for the waveguide created, clearly indicating the presence of a confined beam.

According to Equations (1) and (2), the refractive index change (Δn) at 632 nm was determined. The exposed area to the fs laser, which is the focal region of the written lines, showed a negative refractive index change. This resulted in the surrounding glass remaining unaffected. Consequently, the unaffected central region became the core of the waveguide, effectively confining light. The Δn values for both, x and y - directions were of the order of 10^{-3}.

Fig. 6 (a) and (b) show the results of the beam waist (d = 2w) as a function of the position z and the results of M^2 at 632 nm obtained using Equation (3) for the horizontal and vertical axes ($M_x^2 = 7.52$ and $M_y^2 = 7.00$), respectively. M_x^2 and M_y^2 at 1064 nm were computed by using Equation (4), whose results were 4.46 and 4.15, respectively. It was observed that more similar values in the horizontal and vertical directions were achieved at 632 and 1064 nm for eight superimposed lines.

As per the procedure mentioned before, the propagation losses (α) were evaluated using Equation (6) and the value recorded at 1064 nm was 0.44 dB/cm and 0.55 dB/cm for sample without and with Au NPs, respectively.

In order to show evidence of guiding within the written waveguides, pictures were taken from the glass surface as shown in Fig. 8. For better visualization of the guided beam, a piece of white paper was placed on the glass surface and the 632 nm laser was coupled to the waveguide (Fig. 7(a)), showing clear evidence that guidance occurs. However, as shown in Fig. 7 (b), when the sample was positioned so that there was no

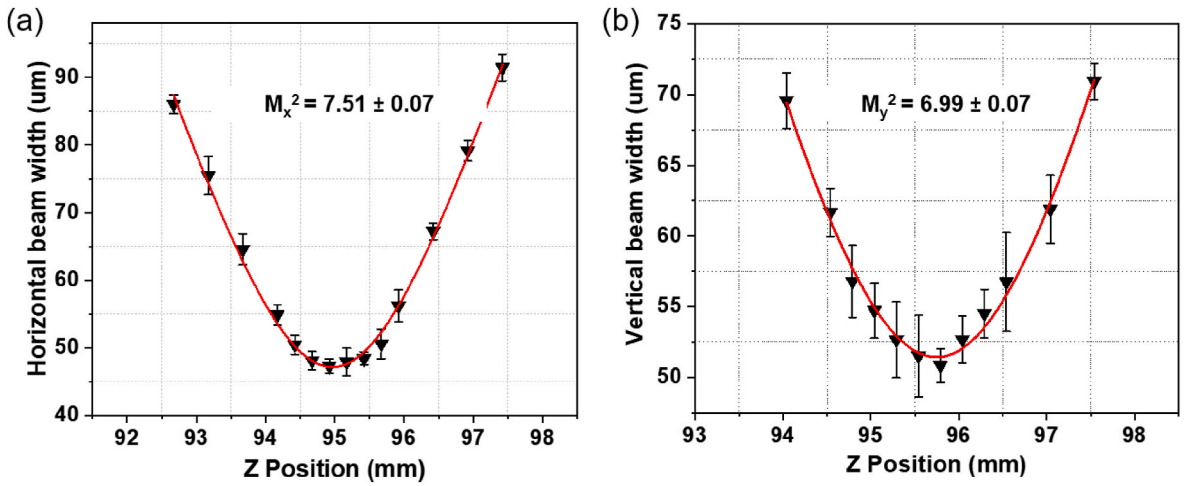

Fig. 6. Results of M_x^2 and M_y^2 at 632 nm for the fs laser irradiation for 8 superimposed lines.

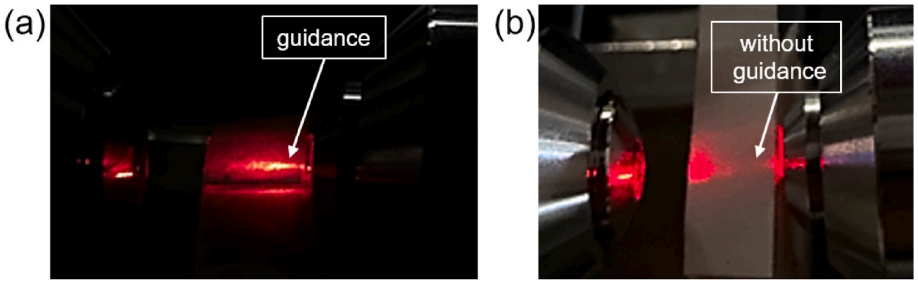

Fig. 7. Pictures of the sample surface. (a) With 632 nm laser coupled to the double guide and (b) with the 632 nm laser irradiated outside the double guide.

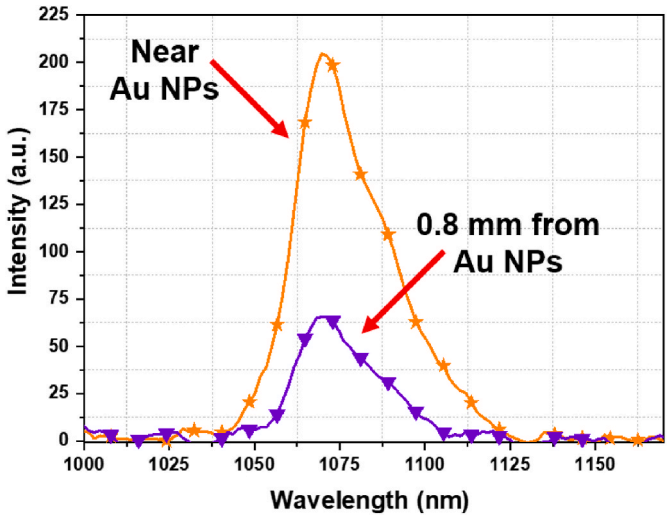

Fig. 8. Photoluminescence results of Nd^{3+} doped GeO_2-PbO glass with Au NPs islands, measured at two different distances: at 0.8 mm from Au NPs (triangle) and close to them (stars), under excitation at 808 nm.

light coupling in the double waveguide, no light guiding was observed on the surface. These images corroborate the presence of the waveguide on the glass surface, where the Au NPs islands are deposited.

Fig. 8 shows the PL of Nd^{3+} doped GeO_2-PbO sample excited at 808 nm. The band centered at 1064 nm is due to the transition $^4F_{3/2} \rightarrow {}^4I_{11/2}$ of Nd^{3+} ions. This result shows the variation of the emission intensity, at 1064 nm, for two different heights of the sample: at 0.8 mm from Au NPs deposited on the surface of the glass and close to them. The highest intensity occurs in the vicinities of the Au NPs islands where we observe PL increase of ~210 % with respect to the result at a longer distance (0.8 mm from Au NPs).

Fig. 9 shows the influence of Au NPs islands on the relative gain at 1064 nm, for measurements performed in glasses with and without the layer of Au NPs islands. The maximum relative gain of 3.0 dB/cm was obtained for the sample with Au NPs islands, corresponding to an increase of ~450 % when compared to the one without Au NPs. The procedure used to determine the relative gain was presented in section 2; Fig. 9 (c) presents the normalized ASE spectrum for pump power at 808 nm (continuous line) and the signal at the waveguide output after ASE removal corresponds to SE signal (dashed line). The input signal at 1064 nm was maintained at very low level (2.8 μW) to avoid gain saturation.

This gain increase is correlated to the local field growth generated in the vicinity of the Au NPs, which enhances the density of excited Nd^{3+} ions. The interaction between metallic NPs and the electromagnetic field leads to the collective oscillation of free electrons and charge separation, the surface plasmon resonance. A dipole is created in the NP and an intense field, referred to as the local field, concentrates around its vicinities, extending from the positive pole to the negative one, promoting the luminescence enhancement of the rare-earth ions located in the neighborhood of the metallic NPs. Similar phenomenon was observed by our group in recent works with waveguides produced using GeO_2-PbO thin films doped with Tm^{3+}/Yb^{3+} and Er^{3+}/Yb^{3+} ions with Au NPs deposited on the waveguide core [30,31]. Pillonnet et al. [36] studied the effect on the luminescence of rare-earth ions caused by the distance between silver metallic NPs and Eu^{3+} ions. Thin layers of Y_2O_3 and Eu:Y_2O_3 were then deposited. The equivalent thickness of the Eu:Y_2O_3 layer was kept constant (10 nm), while the thickness of the spacer layer Y_2O_3 was varied from 0 to 90 nm, corresponding to the distance (d). The results showed that the highest intensity of Eu^{3+} ion emission occurs at a

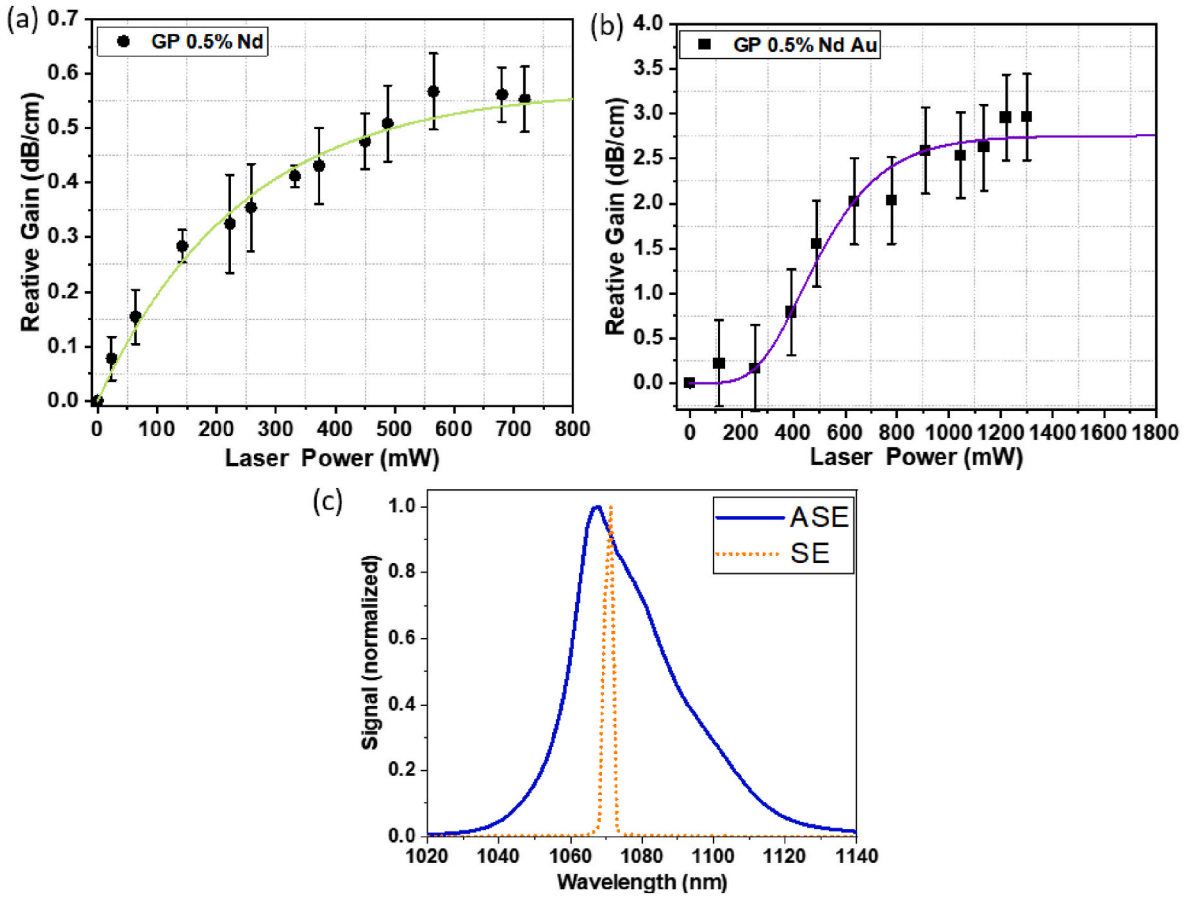

Fig. 9. Relative gain (signal enhancement) at 1064 nm as a function of pump power at 808 nm for the double waveguides written in Nd^{3+}-doped GeO_2-PbO without (a) and with (b) Au NPs (Au NPs were deposited on top of the waveguides that are on the surface of the glass); (c) normalized ASE spectrum for 808 nm pump power, at 222 mW (continuous line) and the SE signal (dashed line), using 2.8 μW of input signal power, at 1064 nm. The waveguides were positioned on the glass surface.

distance of 20 nm from the layer of silver NPs. For values greater than 20 nm, there was a quenching of luminescence. So the position of the waveguides on the glass surface where the Au NPs islands are deposited favored obtaining the positive contribution of the plasmonic effects of Au NPs, leading to the relative gain enhancement of about 450 % at 1064 nm.

Table 1 summarizes the results of Δn, propagations losses, relative gain and M_x^2 and M_y^2.

4. Conclusion

This study explores the influence of Au NPs on the optical properties of Nd^{3+}-doped GeO_2-PbO glass, with double-line waveguides inscribed directly into the glass, 0.7 mm beneath its surface, using a Ti:sapphire laser operating at 808 nm. The dual-line structure was composed of two closely spaced parallel lines, each line being the cumulative result of the superposition of eight individual lines. This procedure was adopted due to previous results with Nd^{3+}-doped GeO_2-PbO glass containing Ag NPs. The sputtering technique was employed to deposit Au on the surface of the double waveguide to study the influence on the optical properties of Nd^{3+}-doped GeO_2-PbO glass. Au NP islands with a size distribution ranging from 5 to 45 nm were observed by atomic force microscopy. Additional procedures were undertaken to position the waveguides on the glass surface where Au NPs are positioned.

The investigation revealed refractive index change of 10^{-3} at 632 nm in both horizontal and vertical directions. Beam quality factors (M_x^2 and M_y^2) at 632 nm and 1064 nm showed similar results and demonstrated x, y-symmetrical guiding in both cases.

In the vicinities of the Au NPs it was observed photoluminescence growth of ~210 % with respect to the result at a longer distance, situated at 0.8 mm from the metallic NPs. We highlight that the relative gain reached 3.0 dB/cm representing an increase of approximately 450 % when compared to the sample without the Au NPs and was attributed to the local field growth in their vicinities. Positioning the waveguides on the glass surface where the Au NPs islands are deposited allowed the positive contribution of the plasmonic effects of the metallic NPs.

As far as we know, this is the first time that the plasmonic effects are observed in Nd^{3+} doped PbO-GeO_2 glasses in waveguides written with fs laser and with Au NPs deposition at the bulk surface.

The present results are relevant for the development of optical amplifiers and can be used in integrated optics in the future.

Table 1
Results of M_x^2, M_y^2, Δn_x, Δn_y, propagation losses and relative gain.

Parameters	Values
Δn_x	5.85×10^{-3}
Δn_y	5.22×10^{-3}
M_x^2 (632 nm)	7.51
M_y^2 (632 nm)	6.99
M_x^2 (1064 nm)	4.46
M_y^2 (1064 nm)	4.15
Relative Gain (dB/cm) – without Au NPs	0.55
Relative Gain (dB/cm) – with Au NPs	3.0
Propagation loss (dB/cm) – without Au NPs	0.44
Propagation loss (dB/cm) – with Au NPs	0.55

CRediT authorship contribution statement

Camila D.S. Bordon: Conceptualization, Methodology, Investigation, Data curation, Writing - Original Draft, Writing – review & editing. **Jessica Dipold:** Methodology, Investigation, Data curation, Writing - Original Draft, Writing – review & editing. **Thiago F. Vecchi:** Investigation, Writing – review & editing. **Niklaus U. Wetter:** Conceptualization, Resources, Writing - Original Draft, Writing – review & editing, Supervision, Project administration, Funding acquisition. **Wagner de Rossi:** Conceptualization, Resources, Writing - Original Draft, Writing – review & editing, Funding acquisition. **Anderson Z. Freitas:** Resources, Writing - Original Draft, Writing – review & editing, Funding acquisition. **Luciana R.P. Kassab:** Conceptualization, Resources, Writing - Original Draft, Writing – review & editing, Supervision, Project administration, Funding acquisition.

Declaration of competing interest

The authors declare that they have no known competing financial interests or personal relationships that could have appeared to influence the work reported in this paper.

Data availability

Data will be made available on request.

Acknowledgments

This work was supported by Coordenação de Aperfeiçoamento de Pessoal de Nível Superior (CAPES-PROEX/88887.495886/2020-00), Conselho Nacional de Desenvolvimento Científico e Tecnológico: National Institute of Photonics (Grant: INCT de Fotônica/465.763/2014); Sisfóton Grant 440.228/2021-2 and Grant: 305745/2023-9, and IPEN/CNEN 2020.06.IPEN.33.PD. The authors thank Fundação de Amparo à Pesquisa do Estado de São Paulo—Grants: FAPESP 2018/19240-5 and 2021/04334-7.

References

[1] K. Walter, Solid-state Laser Engineering, Springer, 2013.
[2] D.G. Lancaster, V.J. Stevens, V. Michaud-Belleau, S. Gross, A. Fuerbach, T. M. Monro, Holmium-doped 2.1 μm waveguide chip laser with an output power> 1 W, Opt Express 23 (2015) 32664–32670, https://doi.org/10.1364/OE.23.032664.
[3] K.M. Davis, K. Miura, N. Sugimoto, K. Hirao, Writing waveguides in glass with a femtosecond laser, Opt. Lett. 21 (1996) 1729–1731, https://doi.org/10.1364/OL.21.001729.
[4] G.F. Almeida, J.M. Almeida, R.J. Martins, L. De Boni, C.B. Arnold, C.R. Mendonca, Third-order optical nonlinearities in bulk and fs-laser inscribed waveguides in strengthened alkali aluminosilcate glass, Laser Phys. 28 (2017) 015401, https://doi.org/10.1088/1555-6611/aa8ac2.
[5] K. Miura, J. Qiu, H. Inouye, T. Mitsuyu, K. Hirao, Photowritten optical waveguides in various glasses with ultrashort pulse laser, Appl. Phys. Lett. 71 (1997) 3329–3331, https://doi.org/10.1063/1.120327.
[6] J.M. Almeida, R.D. Fonseca, L. De Boni, A.R.S. Diniz, A.C. Hernandes, P. H. Ferreira, C.R. Mendonca, Waveguides and nonlinear index of refraction of borate glass doped with transition metals, Opt. Mater. (2015) 522–525, https://doi.org/10.1016/j.optmat.2015.01.048.
[7] L.B. Fletcher, J.J. Witcher, N. Troy, S.T. Reis, R.K. Brow, D.M. Krol, Effects of rare-earth doping on femtosecond laser waveguide writing in zinc polyphosphate glass, J. Appl. Phys. 112 (2012) 023109, https://doi.org/10.1063/1.4739288.
[8] P. Nandi, G. Jose, C. Jayakrishnan, S. Debbarma, K. Chalapathi, K. Alti, A. K. Dharmadhikari, J.A. Dharmadhikari, D. Mathur, Femtosecond laser written channel waveguides in tellurite glas, Opt Express 14 (2006) 12145–12150, https://doi.org/10.1364/OE.14.012145.
[9] T.T. Fernandez, S.M. Eaton, G. Della Valle, R.M. Vazquez, M. Irannejad, G. Jose, A. Jha, G. Cerullo, R. Osellame, P. Laporta, Femtosecond laser written optical waveguide amplifier in phospho-tellurite glass, Opt Express 18 (2010) 20289–20297, https://doi.org/10.1364/OE.18.020289.
[10] M.P. Smayev, V.V. Dorofeev, A.N. Moiseev, A.G. Okhrimchuk, Femtosecond laser writing of a depressed cladding single mode channel waveguide in high-purity tellurite glass, J. Non-Cryst. 480 (2018) 100–106, https://doi.org/10.1016/j.jnoncrysol.2017.11.007.
[11] D.S. da Silva, N.U. Wetter, W. de Rossi, L.R.P. Kassab, R.E. Samad, Production and characterization of femtosecond laser-written double line waveguides in heavy metal oxide glasses, Opt. Mater. 75 (2018) 267–273, https://doi.org/10.1016/j.optmat.2017.10.033.
[12] M. Khalid, G.Y. Chen, J. Bei, H. Ebendorff-Heidepriem, D.G. Lancaster, Microchip and ultra-fast laser inscribed waveguide lasers in Yb^{3+} germanate glass, Opt. Matter. 9 (2019) 3557–3564, https://doi.org/10.1364/OME.9.003557.
[13] D.S. Da Silva, N.U. Wetter, L.R.P. Kassab, W. De Rossi, M.S. De Araujo, Double line waveguide amplifiers written by femtosecond laser irradiation in rare-earth doped germanate glasses, J. Lumin. 217 (2020), https://doi.org/10.1016/j.jlumin.2019.116789.
[14] J.P. Bérubé, A. Le Camus, S.H. Messaddeq, Y. Petit, Y. Messaddeq, L. Canioni, R. Vallée, Femtosecond laser direct inscription of mid-IR transmitting waveguides in BGG glasses, Opt. Mater. Express 7 (2017) 3124–3135.
[15] M. Hongisto, A. Veber, Y. Petit, T. Cardinal, S. Danto, V. Jubera, L. Petit, Radiation-induced defects and effects in germanate and tellurite glasses, Materials 13 (2020) 3846, https://doi.org/10.3390/ma13173846.
[16] A.P. Kumar, S.H. Bindu, P.V. Rao, R. Klement, D. Galusek, N. Veeraiah, P.S. Prasad, Enhancement of rare earth ions hosting potential of B_2O_3 added germanium based glasses: a detailed optical analysis, J. Alloys Compd. 883 (2021) 160800, https://doi.org/10.1016/j.jallcom.2021.160800.
[17] J. Wang, J.R. Lincoln, W.S. Brocklesby, R.S. Deol, C.J. Mackechnie, A. Pearson, A. C. Tropper, D.C. Hann, D.N. Payne, Fabrication and optical properties of lead-germanate glasses and a new class of optical fibers doped with Tm^{3+}, J. Appl. Phys. 73 (1993) 8066–8075, https://doi.org/10.1063/1.353922.
[18] J. Yang, K. van Dalfsen, K. Worhoff, F. Ay, M. Pollnau, High-gain Al_2O_3: Nd^{3+} channel waveguide amplifiers at 880 nm, 1060 nm, and 1330 nm, Appl. Phys. B 101 (2010) 119–127, https://doi.org/10.1007/s00340-010-4001-2.
[19] X. Long, J. Bai, X. Liu, W. Zhao, G. Cheng, Buried waveguide in neodymium-doped phosphate glass obtained by femtosecond laser writing using a double line approach, Chin. Opt Lett. 11 (2013) 102301. https://opg.optica.org/col/abstract.cfm?URI=col-11-10-102301.
[20] G. Matthäus, J. Burghoff, M. Will, S. Nolte, A. Tünnermann, Thermal effects vs. gain in femtosecond laser written waveguides in neodymium doped fused silica, Appl. Phys. A 83 (2006) 347–350, https://doi.org/10.1007/s00339-006-3560-x.
[21] C. Miese, S. Gross, M.J. Withford, A. Fuerbach, Waveguide inscription in Bismuth Germanate crystals using high repetition rate femtosecond lasers pulses, Opt. Mater. Express 5 (2015) 323–329, https://doi.org/10.1364/OME.5.000323.
[22] J.M. Oliveira, A.J. Jesus-Silva, A.C. Silva, N.O. Dantas, E.J. Fonseca, Waveguides written in silver-doped tellurite glasses, Opt. Mater. 101 (2020) 109767, https://doi.org/10.1016/j.optmat.2020.109767.
[23] C.D. Bordon, J. Dipold, A.Z. Freitas, N.U. Wetter, W. de Rossi, L.R.P. Kassab, A new double-line waveguide architecture for photonic applications using fs laser writing in Nd^{3+} doped GeO_2-PbO glasses, Opt. Mater. 129 (2022) 112495, https://doi.org/10.1016/j.optmat.2022.112495.
[24] C.D.S. Bordon, J. Dipold, N.U. Wetter, W. de Rossi, A.Z. Freitas, L.R. Kassab, Effect of silver nanoparticles on the optical properties of double line waveguides written by fs laser in Nd^{3+}-doped GeO_2-PbO glasses, Nanomaterials 13 (2023) 743, https://doi.org/10.3390/nano13040743.
[25] P. Anger, P. V, L. Novotny, Enhancement and quenching of single-molecule fluorescence, Phys. Rev. Lett. 96 (2006) 113002, https://doi.org/10.1103/PhysRevLett.96.113002.
[26] J.A. Schuller, E.S. Barnard, W. Cai, Y.C. Jun, J.S. White, M.L. Brongersma, Plasmonics for extreme light concentration and manipulation, Nat. Mater. 9 (2010) 193–204, https://doi.org/10.1038/nmat2630.
[27] C. Yu, Z. Yang, J. Zhao, A. Huang, J. Qiu, Z. Song, D. Zhou, B. Liu, Preparation and photoluminescence enhancement of Au nanoparticles with ultra-broad plasmonic absorption in glasses, J. Am. Ceram. Soc. 102 (2019) 4200–4212, https://doi.org/10.1111/jace.16300.
[28] B.N. Swetha, K. Keshavamurthy, G. Gupta, D.A. Almuqrin, A.H. Sayyed, M. I. Aloraini, G. Jagannath, Silver nanoparticles enhanced photoluminescence and the spectroscopic performances of Nd^{3+} ions in sodium lanthanum borate glass host: effect of heat treatment, Ceram. Int. 47 (2021) 21212–21220, https://doi.org/10.1016/j.ceramint.2021.04.124.
[29] M. Reza Dousti, Efficient infrared-to-visible upconversion emission in Nd^{3+}-doped PbO-TeO_2 glass containing silver nanoparticles, J. Appl. Phys. 114 (2013) 113105, https://doi.org/10.1063/1.4821430.
[30] T.A.A. de Assumpção, M.E. Camilo, M.I. Alayo, D.M. da Silva, L.R.P. Kassab, Influence of gold nanoparticles on the 805 nm gain in Tm^{3+}/Yb^{3+} codoped PbO-GeO_2 pedestal waveguides, Opt. Mater. 72 (2017) 518–523, https://doi.org/10.1016/j.optmat.2017.06.031.
[31] F.A. Bomfim, R.C. Rangel, D.M. da Silva, D.O. Carvalho, E.G. Melo, M.I. Alayo, L. R. Kassab, A new fabrication process of pedestal waveguides based on metal dielectric composites of Yb^{3+}/Er^{3+} codoped PbO-GeO_2 thin films with gold nanoparticles, Opt. Mater. 86 (2018) 433–440, https://doi.org/10.1016/j.optmat.2018.10.044.
[32] A.K. Ghatak, K. Thyagarajan, An Introduction to Fiber Optics, Cambridge university press, 1998.
[33] A.E. Siegman, Defining and measuring laser beam quality, in: M. Inguscio, R. Wallenstein (Eds.), Solid State Lasers: New Developments and Applications, Springer, Boston, MA, 1993, pp. 13–28, https://doi.org/10.1007/978-1-4615-2998-9_2.

[34] D. Feise, G. Blume, H. Dittrich, C. Kaspari, K. Paschke, G. Erbert, High-brightness 635nm tapered diode lasers with optimized index guiding, Proc. SPIE 7583 (2010) 75830V, https://doi.org/10.1117/12.840658, 1-75830V-12.
[35] D.L. Yang, E.Y.B. Pun, B.J. Chen, H. Lin, Radiative transitions and optical gain in Er^{3+}/Yb^{3+} codoped acid-resistant ion exchanged germanate glass channel waveguides, J. Opt. Soc. Am. B 26 (2009) 357–363, https://doi.org/10.1364/JOSAB.26.000357.
[36] A. Pillonnet, A. Berthelot, A. Pereira, O. Benamara, S. Derom, G. Colas des Francs, A.M. Jurdyc, Coupling distance between Eu^{3+} emitters and Ag nanoparticles, Appl. Phys. Lett. 100 (2012) 153115, https://doi.org/10.1063/1.3703120.